Lab on a Chip

PAPER

Nuclear deformation during breast cancer cell transmigration†‡

Yi Fu,[abc] Lip Ket Chin,[a] Tarik Bourouina,[c] Ai Qin Liu[a] and Antonius M. J. VanDongen*[b]

Metastasis is the main cause of cancer mortality. During this process, cancer cells dislodge from a primary tumor, enter the circulation and form secondary tumors in distal organs. It is poorly understood how these cells manage to cross the tight syncytium of endothelial cells that lines the capillaries. Such capillary transmigration would require a drastic change in cell shape. We have therefore developed a microfluidic platform to study the transmigration of cancer cells. The device consists of an array of microchannels mimicking the confined spaces encountered. A thin glass coverslip bottom allows high resolution imaging of cell dynamics. We show that nuclear deformation is a critical and rate-limiting step for transmigration of highly metastatic human breast cancer cells. Transmigration was significantly reduced following the treatment with a protein methyltransferase inhibitor, suggesting that chromatin condensation might play an important role. Since transmigration is critical for cancer metastasis, this new platform may be useful for developing improved cancer therapies.

Introduction

Cell migration across a cellular barrier, *i.e.* transmigration, plays critical roles in multiple biological processes, including tissue morphogenesis, immune response and cancer metastasis.[1–3] During metastasis, cancer cells leave the primary site and migrate through the vascular system to new sites, where they establish distant colonies. When entering (intravasation) and exiting (extravasation) the vascular vessel, cancer cells need to transmigrate across the endothelial layer and the underlying basement membranes of the vessel walls.[4,5] The stiffness and geometry confinement of the cellular barriers creates serious challenges to the cancer cells, which require them to sustain drastic deformations during the transmigration process.[6,7] As the largest organelle in the cell, the nucleus consists of dense genetic materials surrounded by a lipid bilayer envelope supported by a network of structural proteins. Biophysical studies have shown that the nucleus is 5 to 10-fold stiffer than the surrounding cytoplasm.[8] Although previous studies on cancer metastasis have shown that the nucleus might be the rate-limiting organelle,[9,10] the dynamics of the cancer cell and its nucleus during transmigration has not been characterized and their importance remains unascertained.

Chromatin occupies a substantial volume of the nucleus. It consists of repetitive units of DNA wrapped around histone

octamers, forming flexible structures. Chromatin responds dynamically to various external and internal biological signals by switching between two morphological states: (1) condensed heterochromatin and (2) open euchromatin, through the concerted action of post-translational modifications on the histone tails.[11,12] Changes in the chromatin condensation state may result in altering of the mechanical properties of the nucleus.[13] Since drastic changes in nuclear shape are likely during the transmigration process, we asked whether they are associated with changes in the chromatin condensation state. If changes in the chromatin structure do occur and they can be shown to play a critical role in the transmigration process, then novel strategies for preventing and inhibiting cancer metastasis could be developed. Pharmacological or biological approaches that target the processes underlying nuclear deformation may inhibit the transmigration of cancer cells and subsequently reduce their metastatic capabilities.

Most of the studies on cancer cell transmigration have been performed on traditional platforms, including the Boyden chamber and the Matrigel migration assay.[14,15] Although numerous results have been obtained on these platforms, they are still lacking several important capabilities, including the control and standardization of micro-environmental parameters, high-resolution imaging of cellular components and real-time monitoring of transmigration. With advances in miniaturization and microfabrication technologies, engineers have developed novel devices capable of overcoming the shortages of these traditional platforms.[16–18] With these innovations, the study of cell transmigration has been brought to a higher level.

In recent years, biologists have begun to use these new platforms to study the roles of individual cellular components in cellular transmigration. While most of the studies have focused on motor proteins and cytoskeleton-related components such as

[a]School of Electrical and Electronic Engineering, Nanyang Technological University, Singapore, 639798
[b]Duke-NUS Graduate Medical School, Singapore, 169857.
E-mail: antonius.vandongen@duke-nus.edu.sg; Fax: +65 6557-0729; Tel: +656516-7075
[c]Ecole Supérieure d'Ingénieurs en Electronique et Electrotechnique, Université Paris-Est, Paris, 93162, France
† Published as part of a themed issue on optofluidics.
‡ Electronic supplementary information (ESI) available.

myosin and keratin,[19,20] few have addressed factors related to cellular deformation, which is likely to occur during transmigration. In this paper, we investigate changes in cellular and nuclear morphology associated with the transmigration process, using highly metastatic human breast cancer cells MDA-MB-231 growing in a microfluidics device. Morphological changes of the cell nucleus and its relative positioning within the cell were recorded during the migration process. The transmigration profile of MDA-MB-231 cells was compared with that of MCF-7 cells, human breast cancer cells, which are poorly metastatic. To address the importance of the chromatin condensation status in transmigration, a chromatin de-condensation drug, 5′-deoxy-5′-methylthioadenosine was introduced to cancer cells, and its effect on the prevention of cancer cell transmigration was studied.

Materials and methods

Design and fabrication of microfluidic device

A schematic illustration of the microfluidic transmigration device is shown in Fig. 1. The microfluidic chip is made of Polydimethylsiloxane (PDMS). It consists of two chambers, which are linked by an array of microchannels with a height of 5 μm, a length of 100 μm and widths ranging from 4 to 12 μm. The microchannels are designed to mimic small gaps in the extracellular matrix and epithelial syncytium, encountered by the cancer cells during their transmigration, as they enter and exit the circulation. The widths of the microchannels (4–12 μm) are designed to allow only single cells to migrate. The average diameter of an MDA-MB-231 cell nucleus is 6–8 μm. When the cells are transmigrating through a narrow microchannel, a geometric constriction will be imposed on their shape. The viscoelastic property of the cell nucleus and the stiffness of PDMS will result in nuclear deformation.

The device is fabricated using standard soft-lithography techniques.[21] A two-step photolithography method was used in the fabrication process. First, a 5-μm thin layer of SU-8 photoresist (SU-10, MicroChem) was spin-coated on a silicon

Fig. 1 A schematic illustration of the microfluidic transmigration device, which consists of two chambers interconnected by an array of microchannels with a height of 5 μm, a length of 100 μm and widths ranging from 4–12 μm. Cells are seeded and grown in the cell culture chamber. When a chemoattractant is applied to the chemoattractant chamber, a concentration gradient is established along the microchannels, which induces the cancer cells to migrate through the microchannels.

wafer (CEE 200, Brewer Science). After soft baking, it was exposed with the first chrome mask, which patterned the microchannel, and this was followed by the post exposure bake. After development, a second 100-μm thick layer of SU-8 (SU-100, MicroChem) photoresist was spin-coated on top of the first layer and exposed with a second mask to pattern the cell culture chambers and the chemoattractant chamber. PDMS (Sylgard 184, Dow Corning) prepolymer and curing agent mixture (10 : 1) was poured over the silicon master, degassed, baked for 2 h at 75 °C and then peeled off. The inlet and outlet holes were punched manually using a Harris uni-core sampling puncher. Then, the PDMS devices were exposed to air plasma for 15 s using a corona treater (BD-25, Electro-Technic Products) and bonded with a glass coverslip. Transparency of the PDMS material and the thin glass coverslip on the bottom allowed us to track the morphological changes of cells when they were migrating through precisely defined structures.[22] Cells could be seeded and cultivated in the device under normal cell culture conditions.

Cell culture

Reagents for cell culture were purchased from Invitrogen. Human breast cancer cells (MDA-MB-231) were maintained in Dulbecco's modified Eagle's medium, supplemented with 10% fetal bovine serum (FBS) and 1% penicillin/streptomycin (P/S) at 37 °C and 5% CO_2. The human breast cancer cell line MCF7 was maintained in minimum essential medium supplemented with 10% FBS, 1% P/S and 0.01 mg ml^{-1} bovine insulin at 37 °C and 5% CO_2.

Transmigration in the microfluidic device

To enhance cell attachment and migration, 50 μg ml^{-1} of fibronectin (Sigma) was injected into the PDMS chip and incubated overnight at 4 °C. The fibronectin solution was then removed and the microchannels were flushed 3 times with phosphate-buffered saline (PBS). Adherent cells from the culture flask were detached by trypsin/EDTA treatment, spun down and resuspended in growth medium at a density of 10^7 cells ml^{-1}. To stain the nuclei of the cells, fluorescent dye Hoechst 33342 (Invitrogen) was added to the cell suspension at a concentration of 1 μg ml^{-1} and incubated at 37 °C for 30 min. Cells were then injected into the cell culture chamber and incubated at 37 °C for 2 h to allow the cells to attach to the substrate and spread. The medium in the cell culture chamber was then replaced with a growth medium without serum. The cells were incubated overnight at 37 °C for serum starvation. A complete growth medium supplemented with 20% FBS was then added to the chemoattractant chamber.

Drug experiment

5′-Deoxy-5′-methylthioadenosine (MTA) is a general protein methyltransferase inhibitor, which blocks the transfer of methyl groups to specific lysine residues on histones and consequently inhibits the formation of heterochromatin.[23] A stock solution of MTA (Sigma) was prepared in dimethyl sulfoxide (DMSO) at a concentration of 300 mM. For the treatment of MDA-MB-231 cells, MTA was diluted with the culture medium to a final concentration of 3–300 μM before being loaded into the device.
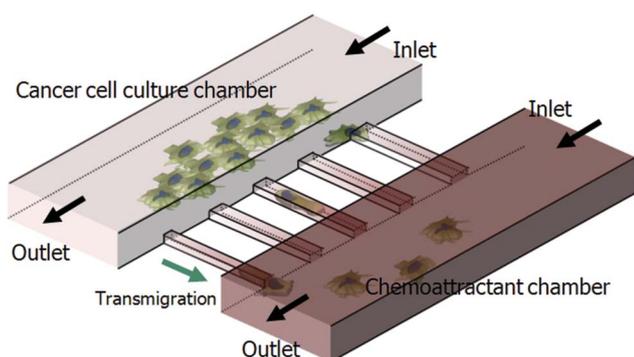
Imaging system and data analysis

The microfluidic device is placed on a motorized Nikon Ti-E microscope equipped with a temperature controlled environmental chamber. Objective lenses used for imaging include Nikon Plan Fluor $10\times$ and $20\times$ dry lenses and a $40\times$ oil lens, with numerical apertures of 0.3, 0.75 and 1.3, respectively. Both digital interference contrast (DIC) and fluorescence images were acquired using a cooled EM-CCD camera (iXon 885, Andor Technology). Fluorescence of the Hoechst 33423 dye was visualized using a DAPI filter set (Chroma Technologies). Time lapse images of the cells in the microchannels were taken during the transmigration process. The captured images were analyzed by the NIS-AR Elements software (Nikon). The transmigration percentage is calculated by the ratio of the number of migrated cells over the total cell population.

Experimental results and discussion

MDA-MB-231 cells transmigration in the microfluidic device

Fig. 2(a) shows an overview of the transmigration of MDA-MB-231 cells in the microfluidic device. After serum starvation in the cell culture chamber and application of FBS to the chemoattractant chamber, a concentration gradient of chemokines in

FBS was established along the microchannels and provided cues for cell transmigration. This is a general behavior of cells commonly known as chemotaxis. When transmigrating through the microchannels, the cells deformed and reshaped based on the geometry of the microchannels, as shown in Fig. 2(b).

Nuclear deformation of cancer cell nucleus during transmigration

Fig. 3(a) shows the transmigration process of MDA-MB-231 cells through the microchannels with a cross-section of $8 \times 5 \mu m$ ($W \times H$). Fluorescently stained nuclei are shown in Fig. 3(b). Images were taken at different time points during the transmigration process. Transmigration occurred in several distinct steps. First, cells came into contact with the entrance of the channel and extended their cytoplasm into it. During this process, the cytoplasm quickly adjusted its shape based on the geometry of the microchannel. It took approximately 30 min for most of the cytoplasm to enter the microchannel, leaving behind the nucleus surrounded by a small amount of cytoplasm. Because of the relatively large nuclear size, cells remained trapped at the entrance. It took much longer (on average 4 h) for the nucleus to deform and allow the entire cell to squeeze into the microchannel. The nucleus deformed from a spherical, to an elongated ellipsoidal shape. After the entire cell has entered the microchannel, the cells migrated at a speed approximately 50 μm h^{-1} towards the chemoattractant chamber. Nuclear dynamics during the process is shown in Movie M1 (ESI‡). These results suggest that deformation of the nucleus is the rate-limiting step during the transmigration process.

The transmigration profiles of MDA-MB-231 and MCF7 for different widths of the microchannels are shown in Fig. 4. Because smaller microchannels require a higher extent of deformation of the nucleus, the percentage of transmigrated cells reduced with decreased microchannel width. For 12 μm wide channels, 36% of the MDA-MB-231 cells migrated across the microchannels in 12 h, after the loading of the chemoattractant.
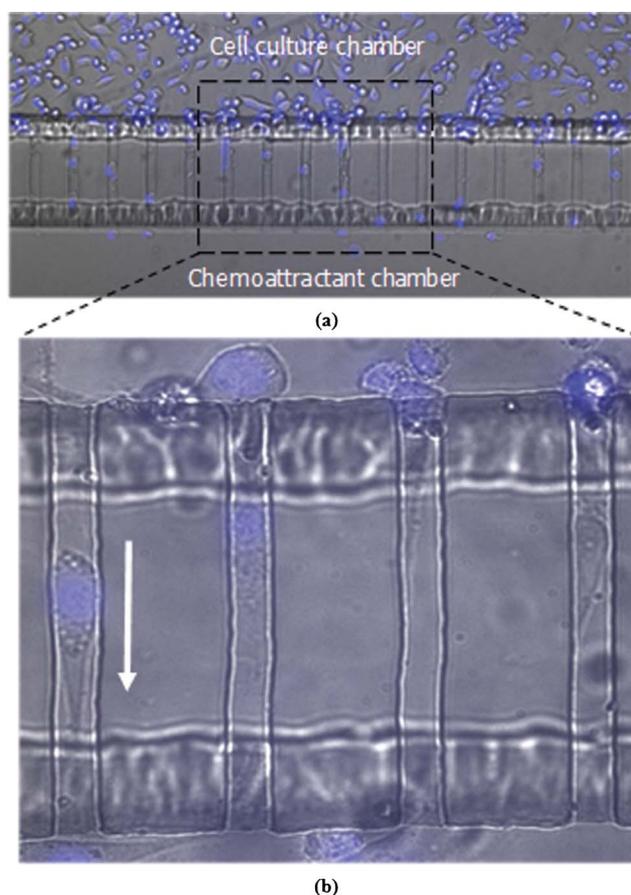

Fig. 2 (a) An overview and (b) zoomed-in view of MDA-MB-231 cells transmigrating in the microfluidic device. Nuclei of the cells were stained with fluorescent dye Hoechst 33423. DIC and fluorescent images (blue) are over-laid.
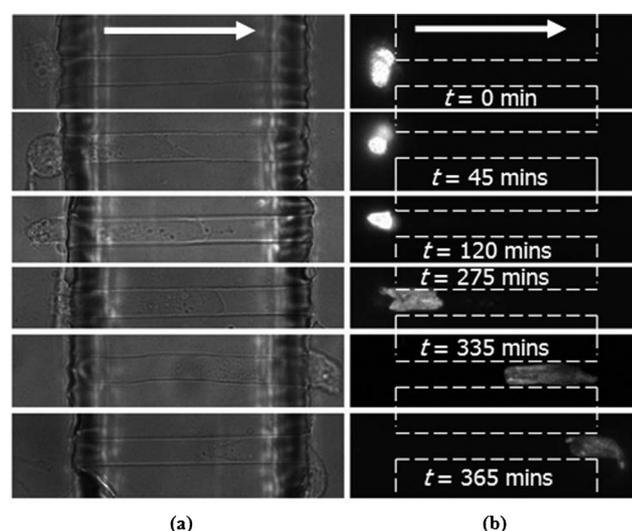

Fig. 3 (a) DIC and (b) fluorescent images showing the migration of MDA-MB-231 cells through an 8 μm wide microchannel. The nucleus of the cell is stained with blue fluorescent dye Hoechst 33423. The elongation and de-condensation of the nucleus in the microchannel are observed.
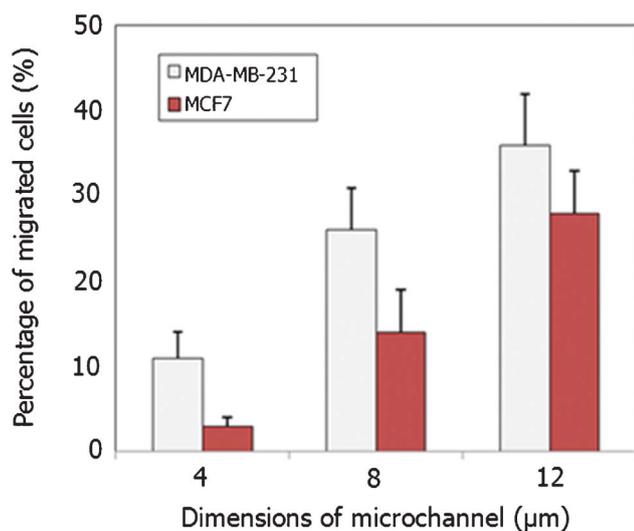
Fig. 4 Transmigration profiles of MDA-MB-231 cells and MCF7 cells in different widths of microchannels.

Fig. 5 The effect of the drug MTA on the transmigration profile of MDA-MB-231 cells in different widths of microchannels.

The number drops significantly to 26% in 8 μm microchannels and 14% in 4 μm microchannels. The transmigration ability of highly metastatic MDA-MB-231 cells was compared with the poorly metastatic MCF7 cells. At each channel dimension, the percentage of transmigrated cells was significantly higher for MDA-MB-231 than for MCF7. The difference was more substantial in narrower microchannels. In 12 μm wide channels, the transmigration rates were 36% *vs.* 28%. However, the migration rate of MDA-MB-231 cells (11%) was almost 3-fold higher than that of MCF7 (4%) in 4 μm wide channels. Transmigration of cancer cells was completely inhibited when the channel width is reduced to 2 μm (see Fig. S1 of ESI‡). Although a direct comparison of the mechanical properties of these two cell types has not yet been performed, the results suggest that MDA-MD-231 cells have a higher deformation capability than MCF7 cells, which might facilitate their transmigration during metastasis.

Chromatin de-condensation with MTA

Transmigration of cancer cells requires a dynamic reshaping of their nuclei. As chromatin fibers occupy a large portion of the nuclear volume,[24] it is possible that reshaping of the nucleus is associated with changes in chromatin architecture. To examine the importance of the chromatin condensation state in the transmigration of cancer cells, MDA-MB-231 cells were treated with MTA, which inhibits the activity of protein methyltransferases, implicated in the formation of heterochromatin. MTA has been shown to cause de-condensation of chromatin. To test the effect of MTA on the overall transmigration profile of the MDA-MB-231 cells in the microchannel array, different concentrations of MTA (0 to 300 μM) were applied. The results are shown in Fig. 5. MTA reduces the transmigration of MDA-MB-231 cells in a concentration-dependent manner. The effects became more significant when the concentration of the MTA was 30 μM or higher and were more obvious in the narrow channels. At the highest applied concentration (300 μM), the migration rates were reduced by 17%, 46% and 64% in the 12, 8 and 4 μm microchannels, respectively. This strong width
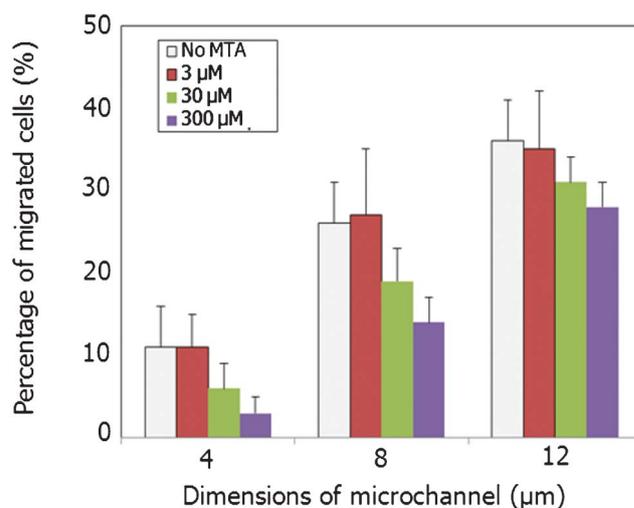
dependence of the MTA effect on transmigration shows that MTA does not restrict cancer cell migration due to cell toxicity. The results, therefore, suggest that MTA impaired the transmigration abilities of cancer cells because de-condensed chromatin induced by MTA makes it difficult for the cell nucleus to become elongated and migrate through the microchannels. In addition to the lower transmigration percentages seen with MTA, some of the cells treated with MTA also migrate slower (<10 μm h^{-1}) than non-treated cells (~ 50 μm h^{-1}, see Movie M2 and M3 of ESI‡).

Because modification of the chromatin condensation status may alter gene transcription profiles and subsequently prevent cancer metastasis, some chromatin-modifying reagents are now being tested in clinical trials as potential anti-cancer drugs.[25] The data presented here suggest that the anti-metastatic properties of these drugs may also be related to additional effects on chromatin stability in resisting nuclear deformation. As chromatin condensation facilitates nuclear reshaping and squeezing during the migration process, chromatin de-condensation by MTA might impede the ability of the nucleus to undergo the structural changes required for the invasion of the metastatic cells through the small gaps in the extracellular matrix and epithelial syncytium.

Conclusions

Nuclear deformation during transmigration of breast cancer cells was studied using a microfluidic transmigration platform. The experimental results show that deformation of cancer cell nuclei is the primary rate-limiting step during the transmigration process. The highly metastatic cancer cell line MDA-MB-231 showed higher nucleus deformation and transmigration capabilities than the poorly metastatic MCF7 cells. The ability of the cell nucleus to squeeze into the microchannels may be related to the chromatin condensation status, since the chromatin de-condensation drug MTA reduced the transmigration efficiency of MDA-MB-231 cells in the microchannels in a width-dependent manner. Because transmigration is a critical process

in cancer metastasis, these results may be useful in developing new anti-cancer strategies.

Acknowledgements

References

1 T. J. Mitchison and L. P. Cramer, *Cell*, 1996, **84**, 371.
2 M. Schindler, J. Ahmed, J. Kamal, A. Nur-E-Kamal, T. H. Grafe, H. Y. Chung and S. Meiners, *Biomaterials*, 2005, **26**, 5624.
3 M. D. Bashyam, *Cancer*, 2002, **94**, 1821.
4 D. R. Sherwood, *Trends Cell Biol.*, 2006, **16**, 250.
5 R. G. Rowe and S. J. Weiss, *Trends Cell Biol.*, 2008, **18**, 560.
6 A. F. Chamber, A. C. Groom and I. C. MacDonald, *Nat. Rev. Cancer*, 2002, **2**, 563.
7 P. Friedl P, *Curr. Opin. Cell Biol.*, 2004, **16**, 14.
8 P. Friedl, K. Wolf and J. Lammerding, *Curr. Opin. Cell Biol.*, 2011, **23**, 55.
9 K. Wolf, Y. I. Wu, Y. Liu, J. Geiger, E. Tam, C. Overall, M. S. Stack and P. Friedl, *Nat. Cell Biol.*, 2007, **9**, 893.
10 C. Beadle C, M. C. Assanah, P. Monzo, R. Vallee, S. S. Rosenfeld and P. Canoll, *Mol. Biol. Cell*, 2008, **19**, 3357.
11 B. D. Strahl and C. D. Allis, *Nature*, 2000, **403**, 41.
12 T. Jenuwein and C. D. Allis, *Science*, 2001, **293**, 1074.
13 J. D. Pajerowski, K. N. Dahl, F. L. Zhong, P. J. Sammak and D. E. Discher, *Proc. Natl. Acad. Sci. U. S. A.*, 2007, **104**, 15619.
14 L. M. Shaw, *Methods Mol. Biol.*, 2005, **294**, 97.
15 J. Banyard and B. R. Zetter, *Cancer Metastasis Rev.*, 1998, **17**, 449.
16 K. C. Chaw, M. Maninaran, E. H. Tay and S. Swaminathan, *Lab Chip*, 2007, **7**, 1041.
17 D. Irimia and M. Toner, *Integr. Biol.*, 2009, **1**, 506.
18 M. L. Heuzé, O. Collin, E. Terriac, A. M. Lennon-Duménil and M. Piel, *Methods Mol. Biol.*, 2011, **769**, 415.
19 M. T. Breckenridge, T. T. Egelhoff and H. Baskaran, *Biomed. Microdevices*, 2010, **12**, 543.
20 C. G. Rolli, T. Seufferlein, R. Kenkemer and J. P. Spatz, *PLoS One*, 2010, **5**, e8726.
21 L. K. Chin, A. Q. Liu, Y. C. Soh, C. S. Lim and C. L. Lin, *Lab Chip*, 2010, **10**, 1072.
22 L. K. Chin, J. Q. Yu, Y. Fu, T. Yu, A. Q. Liu and K. Q. Luo, *Lab Chip*, 2011, **11**, 1856.
23 C. M. Chau and P. M. Lieberman, *J. Virol.*, 2004, **78**, 12308.
24 T. R. Gregory, *Biol. Rev. Cambridge Philos. Soc.*, 2001, **76**, 65.
25 C. B. Yoo and P. A. Jones, *Nat. Rev. Drug Discovery*, 2006, **5**, 37.